

Optical Communications Development for Spacecraft Applications

Bradley G. Boone, Jonathan R. Bruzzi, Bernard E. Kluga, Wesley P. Millard, Karl B. Fielhauer, Donald D. Duncan, Daniel V. Hahn, Christian W. Drabenstadt, Donald E. Maurer, and Robert S. Bokulic

Free-space optical communications systems for deep space and near-terrestrial space environments are now poised for deployment aboard spacecraft. Although many fundamental technical problems have been solved, detailed engineering development is still needed to make space-worthy optical communications terminals. Very high bandwidths (10 Gbps or higher) and fine (1- to 10- μ rad accuracy) pointing systems are needed for near-terrestrial space. For deep space applications, optical links at competitive bandwidths relative to RF systems (e.g., 30 Mbps) with very fine pointing accuracies ($<1 \mu$ rad) are planned. Deep space applications also require very sensitive receivers and large ground receiving apertures, while minimizing mass and prime power penalties for the added capability, especially for smaller spacecraft. Recent efforts at APL focusing on these issues are summarized in this article.

OVERVIEW

Free-space optical communications systems for satellite-to-ground and deep space communications have been proposed, studied, and even implemented in laboratory demonstration systems for more than 30 years. Nevertheless, few of these systems have actually been deployed aboard spacecraft. Even though most of the technical problems associated with optical communications systems have been solved, advances in microwave sources and high-speed electronics have maintained traditional RF communications systems as the technology of choice for space-based communications system designers. This situation is now changing as a

result of several factors: ever-increasing requirements for high data rate (hundreds to thousands of Mbps) communications, significant investments by NASA and DoD, and significant advances in the telecommunications technology for fiber-optic communication components, including fiber amplifiers, fiber lasers, and sensitive receivers. These components may be applicable, in some form, to free-space optical communications systems for use in space.¹ Compact beamsteering technology; very fine pointing, tracking, and stabilization control; and ultra-lightweight antennas are also critical technologies.

The motivation for transitioning to optical communications for deep space applications, apart from pragmatic considerations such as the increasing need to acquire more scientific data and real-time imagery, is fundamentally dependent on the wavelength of light relative to RF bands currently used. As will be described in the section on the link equation, which governs all communications links (both RF and optical), there are three terms that *explicitly* depend on wavelength: the transmitter antenna gain, the space loss, and the receiver antenna gain. When these factors are combined, for equal antenna sizes, the advantages of shorter (optical) wavelengths become obvious: the received signal goes inversely as the square of the wavelength. This is mitigated by the fact that optical antennas are not always as big as RF antennas, and they require greater precision to make and point because of the shortness of the wavelength and the narrowness of the optical beam.

On the other hand, having smaller antennas (as well as other components) can be a weight advantage for optics. Optical modulation bandwidths are also wider because for similar modulation electronics, which are roughly equally limited in their relative (normalized) bandwidths between RF and optical modulators, higher (optical) frequencies directly imply wider bandwidths. This becomes compromised by the fact that, for wider bandwidths (as in optics), in-band noise energy is necessarily greater, thus potentially reducing the signal-to-noise ratio (SNR) for optical receivers.

Complicating the situation, however, are the consequences of a trade between good design practice versus the dominance of photon shot noise in optics and thermal noise in RF systems. Good design in optics drives down the thermal noise so that only the signal-induced (or sometimes the background-induced) shot noise really matters. The real cost of implementing optics on spacecraft over RF systems, however, includes the additional burden of pointing the optical system much more precisely than the RF system. The data rate gain has to offset the additional cost of fine pointing. Most technologists and system developers believe that this trade is now worth it.

APL is developing optical communications system architectures by initially using state-of-the-art commercial off-the-shelf (COTS) components and then replacing them with more advanced and/or innovative technology components as they become available for insertion. The key requirement for optical communications development for space applications is to support science mission data retrieval at higher rates than heretofore possible with RF systems for space missions as far out as interstellar space and all the way in to near-Earth orbit (NEO) or geosynchronous Earth orbit (GEO) distances.

SYSTEM REQUIREMENTS AND FUNCTIONAL ELEMENTS

APL business areas that have supported recent developments include civilian space (for deep space), military space (for near-terrestrial space), and exceptional science and technology (for specific component technologies). Deep space applications being pursued by NASA include the transmission of live video (up to 30 Mbps) from Mars for the Mars Laser Communication Demonstrator planned for a 2009 launch.² GEO ($\approx 36,000$ km) and NEO (≈ 300 – 1000 km) optical communications terminals are also being planned or developed for NASA and DoD. Deep space applications entail a single dedicated channel having a very high pointing accuracy (≈ 300 – 400 nrad) but only a modest data rate (≈ 1 – 30 Mbps, depending on range and background levels). Near-terrestrial space (GEO and NEO) applications will likely involve networked links that will be multichannel and multi-access, require ≈ 1 - to 10 - μ rad pointing accuracies, and entail very high data rates (as much as 10 Gbps or higher). Similar requirements are envisioned for commercial applications. Thus the desired data rates and pointing accuracy requirements are driven by two distinct environments differing mainly in link range. Of course, link margin decreases with range, mainly because laser source power limits and receiver sensitivity constrain the achievable data rate for a desired bit error rate (BER). This is summarized in Fig. 1.

As illustrated in Fig. 2, there are several essential ingredients in a complete end-to-end optical communications system. Besides the communications function, pointing, acquisition, tracking, and stabilization are critical, as are the telescope optics and the

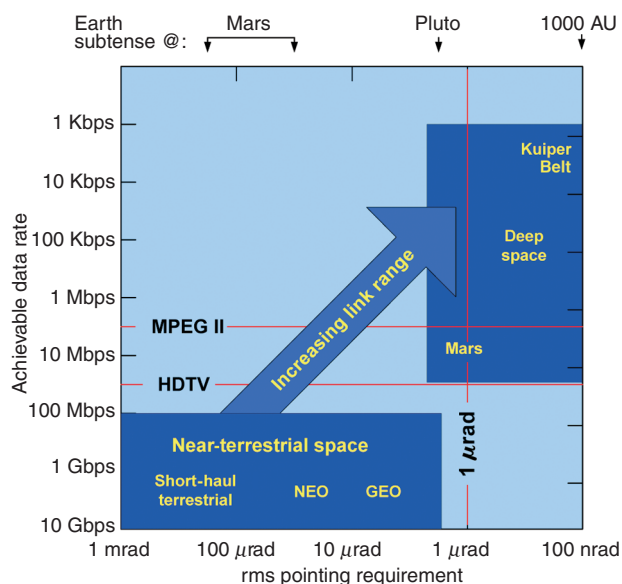


Figure 1. Communications (data rate) and pointing and tracking (rms) accuracy requirements for optical communications to increase link range for a fixed transmitter power.

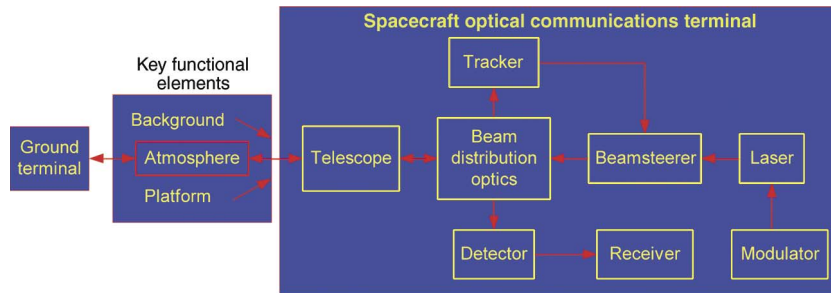


Figure 2. Generic system architecture for an optical communications system.

environmental effects of the atmosphere, background flux, and platform motion. We will describe recent progress at APL addressing most of the technology components and some of the environmental factors.

The Link Equation: Key to System Design and Component Selection

The key relationship between received optical power, P_R and transmitter optical power P_T is given by the link equation (in which all the basic terms are included for an incoherent system):

$$P_R = P_T G_T \eta_T L_{PT} L_{FS} G_R \eta_R L_{PR} L_A,$$

where

$G_T = (\pi D_T / \lambda)^2$ = the gain of the transmitting aperture,

$L_{PT} = \exp(-8\theta^2 / \theta_{div}^2)$ = the pointing loss of the transmitter (assuming a Gaussian-shaped single-mode beam),

$L_{FS} = (\lambda / 4\pi R)^2$ = the free-space propagation loss,

$G_R = (\pi D_R / \lambda)^2$ = the gain of the receiving aperture,

L_{PR} = the pointing loss of the receiver, which is usually negligible,

L_A = the atmospheric attenuation at the operating wavelength,

D_T and D_R = transmitter and receiver apertures, respectively,

R = the link range,
 θ = the beam jitter angle, and

θ_{div} = the optical beam divergence as set by diffraction.

Atmospheric turbulence is not explicitly considered in this simplified link analysis, but it has considerable

impact on receiver performance, especially for links predominantly in the atmosphere.

The link equation also includes other losses that account for imperfect optical components, as denoted by η_T and η_R . These imperfections include losses caused by beam shape, truncation, obscuration, defocusing, obliquity, off-axis positioning (or misalignment), near-field effects, and beamsplitting losses between

the various optical elements in the transmitter and/or receiver. Often for simplicity the incident irradiance is assumed to be due to a diffraction-limited plane wave, which forms a jinc-squared $[2J_1(kr\theta)/kr\theta]^2$ intensity pattern on the detector plane for a single-mode beam. (The jinc-squared shape is characteristic of a light spot produced by a circular aperture, and is defined mathematically as the ratio of the Bessel function of the first kind of order 1 to its argument, where its argument is proportional to displacement from the center of the spot. This shape looks like a sombrero but takes its name *jinc-squared* by analogy with a similar function for a square aperture called the sinc-squared function, where the sinc function is the ratio $\sin x/x$.) Typically, the lack of perfect diffraction is reflected in a wavefront loss factor, $\exp[-(4\pi\sigma/\lambda)^2]$, or Strehl ratio, where the root-mean-square (rms) wavefront error σ should be kept lower than a fraction of a wavelength (at least no greater than $\lambda/4$).

Figure 3 shows how the link equation enters the overall link performance, which includes the detection scheme with its associated noise model and the modulation scheme with its BER. The BER required for the link depends essentially on link distance, desired bit rate, available laser transmitter power, and an estimate of the average number of detected photons per bit at the receiver required for a specified bit error probability. The

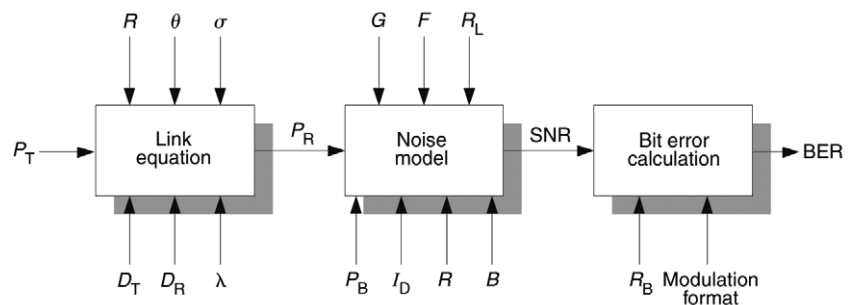


Figure 3. Schematic relationship among transmitter and receiver power, data (or bit) rate (R_B), and bit error rate (BER), as well as the other defining parameters of the system. The link equation, receiver noise model, and BER calculation are the critical factors. In the receiver model, background flux (P_B), photodetector responsivity (R), dark current (I_D), bandwidth (B), noise factor (F), gain (G), and load resistance (R_L) are key parameters.

last factor is usually on the order of 10^{-6} for data rates on the order of 1 Mbps or lower and 10^{-9} for data rates exceeding 100 Mbps.

A study of the current literature indicates the following: for systems that do not contain an optical amplifier, are not background noise limited, and employ a binary signal format, coherent receivers require an average number of detected signal photons/bit on the order of 50, whereas direct-detection intensity-modulated (DD-IM) receivers require an average of roughly 500 detected signal photons/bit to achieve an acceptable BER. (The difference between coherent and incoherent [DD] receivers is that coherent receivers use a local oscillator field to mix with the incoming wavefront before actually detecting their superposition in the photodiode, whereas incoherent receivers merely detect the incoming field directly. In both cases the photodiode is a square-law detector, i.e., it measures the incident light intensity, which is the square of the field.) On the basis of sensitivity, one might choose a coherent detection scheme because it requires fewer photons per bit; however, the atmosphere tends to disrupt the incident beam, causing it to overlap less effectively with the local oscillator beam in coherent receivers. Thus, in practice, it is less problematic to use direct detection. Even without atmospheric turbulence or other disturbances of the incident beam shape, the ideal (quantum) limit for both DD-IM and coherent systems is comparable, on the order of an average of 10 detected signal photons per bit. So, the direct detection scheme is often chosen as a practical matter to minimize system complexity.

Atmospherics: Importance of Cloud-Free Line-of-Sight Statistics

For nearly all applications except deep space, the effects of the Earth's atmosphere must be taken into account. The effects of clouds on optical downlinks (satellite to ground) have been widely recognized. However, the typical approach has been simply to explore the probability of a "cloud-free line of sight." This somewhat ambiguous criterion does not acknowledge that a communications link, albeit at a degraded data rate, could still be established in the presence of clouds of certain optical thicknesses.

To realistically model the effects of clouds on the performance of an optical communications system, we have used existing databases that contain cloud statistics parameterized on optical density.^{3,4} In

conjunction with these statistics, we have used a radiation transport model parameterized on optical thickness that describes the spatio-temporal spreading effects of multiple scattering. Scattering characteristics (scattering and extinction cross sections, and asymmetry parameters) employed in this model are determined from particle size distributions using optical scattering theory. Together, these databases and this model allow link availability probabilities to be derived. Results have been calculated in terms of geographic probability maps of communications at or above prescribed bandwidths, an example of which is shown in Fig. 4.

An optical communications beam is typically incident on a cloud from above, which scatters and absorbs the incident beam. Absorption merely reduces the received power, whereas scatter disperses the beam in angle, spatial extent, and time. The temporal dispersion or pulse stretching is due to the many possible path lengths that a photon can take in traversing the cloud layer. It is this effect that ultimately limits the achievable bandwidth, as it sets the lower limit on the width of the bit slot. The results shown in Fig. 4 have been calculated based on general system parameters chosen to be consistent with technical feasibility (a 1-km-dia. beam footprint at a 1550-nm wavelength and a 20-cm receiver aperture with a 2.5° field of view).

In addition to the effect of clouds and clear air attenuation, atmospheric turbulence causes a significant fluctuation in the angle of arrival of an optical beam, such as a laser, similar to the effect of the atmosphere on a point source, such as a star, causing it to twinkle. This has a significant effect on the achievable bandwidth for uplinks from the ground versus downlinks to the ground, since most of the disturbance in the former case occurs close to the source, whereas in the latter it occurs only

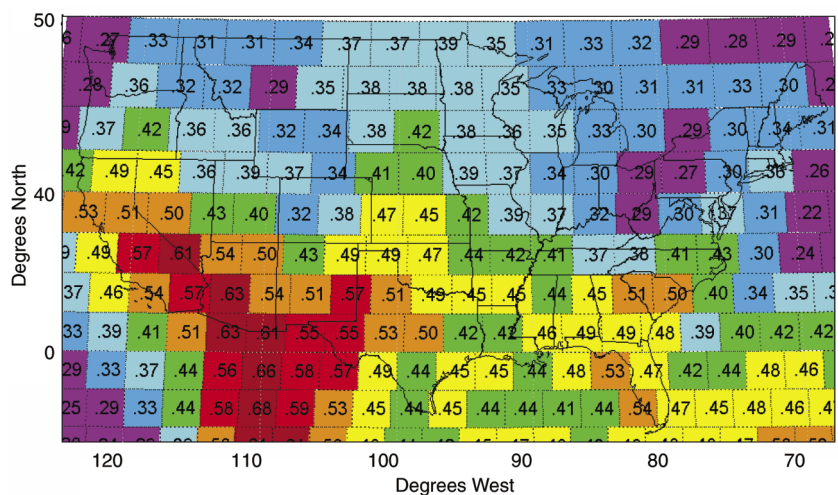


Figure 4. Probability of exceeding a 100-MHz bandwidth over the continental United States for a single site of arbitrary location. Each cell represents an independent weather cell. Weather conditions tend to decorrelate completely over approximately three cells, where an individual cell is ≈ 250 km across.

over the short terminal distance of the atmospheric envelope, especially for deep space links such as those from Mars.

Communications: Pulse Position Modulation Approach

A comparison of coherent (heterodyne detection) and incoherent (DD) receivers generally indicates that for optical communications links through the atmosphere it is better to implement an incoherent DD scheme using an IM laser. The simplest laser transmitter modulation scheme with reasonable design flexibility to meet variable data rate requirements for a variety of deep space missions is the M -ary pulse position modulation (PPM) DD-IM scheme. In this scheme, a single light pulse is transmitted in one of $M = 2^k$ time slots. Hence, each PPM symbol represents $\log_2(M)$ data bits. It is an especially appropriate modulation format when the transmitter is a laser diode. The optimal receiver for this signal format consists of a device that records the number of photons detected in all time slots and places the received PPM light pulse in the time slot that contains the largest of these numbers. Unlike the binary DD-IM on-off keying signaling scheme in which the threshold level for the decision depends on the SNR, the form of the optimal receiver remains the same, even in the presence of noise sources (the performance, of course, does not; it degrades with noise). This signaling scheme was proposed by NASA for deep space communications. This is really about the only realistic possibility for deep space communications with pulsed lasers whose average optical output power is limited to a few watts.

An example PPM transceiver architecture recently developed by APL for spacecraft implementation is illustrated in Figs. 5a and 5b. This breadboard laser transceiver package uses a 4-ary PPM scheme with a field-programmable gate array (FPGA)-based modulator/demodulator.⁵

For the optical transmitter on future spacecraft, we anticipate the use of high-power fiber-amplified lasers. Those with wavelengths around 1060 nm are preferred because it is easier to find sensitive receivers at that wavelength than at the more common 1550-nm wavelength. Although commercial units are readily available, they are not immediately space qualified, nor do they generally meet the mass and power efficiency requirements we desire for spacecraft use. Recent efforts at the Naval Research Laboratory⁶ have resulted in a compact wall-plug-efficient fiber laser with an output power of up to 10 W (continuous wave) and a wall plug efficiency of 40% in a single-mode Gaussian beam. The unit is very compact and attractive for spacecraft use but still requires space qualification, especially to determine its tolerance to radiation.

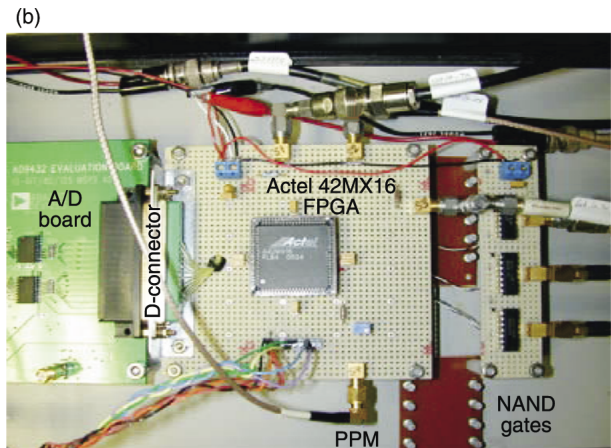
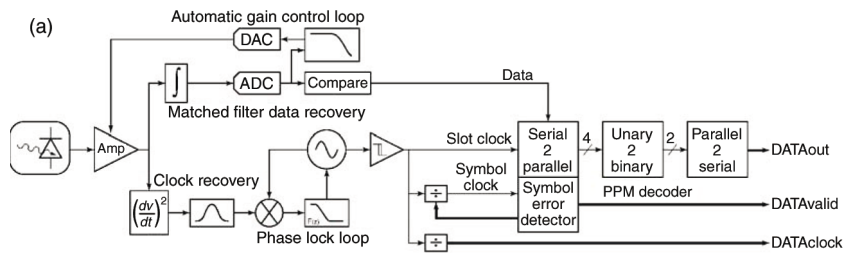


Figure 5. (a) Block diagram of a hybrid (analog/digital) PPM modulator/demodulator and (b) the corresponding field programmable gate array (FPGA) implementation circuit configuration that was tested. This was a preliminary 4-ary configuration for a space-worthy design that will incorporate additional functionality and programmability (e.g., variable M -ary PPM and built-in BER testing).

Compact Beamsteering Technologies for Pointing and Tracking

In light of future developments for deep space optical communications terminals, we have focused on very fine pointing and tracking with accuracies on the order of $1 \mu\text{rad}$ or less and peak-to-peak ranges of $\pm 10 \text{ mrad}$ or more. This translates to an angular dynamic range of at least 40 dB, which is motivated by the desire to body-mount laser transceivers on spacecraft platforms, assuming that spacecraft attitude control systems would have nominally a 10-mrad accuracy for three-axis stabilized attitude control. The maximum permissible pointing error is about one-third of the beamwidth for a single-mode diffraction-limited Gaussian beam. This follows from trading off two terms in the link equation: antenna gain and pointing loss, assuming a Gaussian beam profile. From typical spacecraft platform vibration spectra, as exemplified by the empirical angular deflection data shown in Fig. 6, we can infer that a reasonable rms ($1 - \sigma$) requirement for fine tracking and stabilization for most deep space missions (Mars and beyond) must approach the 300- to 1000-nrad level over a bandwidth approaching 400 Hz.

For these applications it will also be necessary to implement very compact, lightweight, and low-power beamsteering technologies. The most well-developed

and lowest-risk beamsteerers are piezoelectrically driven electromechanical devices. We have tested both macro- and mesoscale beamsteering technologies in which we have used a simple digital servo-controller design in the form of a proportional-integral control system. We have measured and compared the performance of these devices using a quadrant photodiode sensor.^{7,8} The different devices tested are shown in Fig. 7, and their relative performance is summarized in Fig. 8.

In addition to the above technologies, we have also evaluated MEMS (microelectromechanical systems) beamsteering devices, an example of which is shown in Fig. 9a. Micro-mirror technology such as this is applicable to multi-access GEO-to-ground optical communications terminals. For such applications, high-powered laser diodes or laser diode arrays are likely to be sufficient as the transmitter. We are concerned, however, with a number of issues in adapting MEMS technology from fiber-optic communications to free-space optical communications. MEMS mirror shape stability, angular control linearity, dynamic range, and fabrication tolerances are of key concern for their effective application.

Using a MEMX Corp. MEMS micro-mirror, several key performance issues and device parameters were assessed relative to an “ideal” set of requirements. These included the effects of heating caused by incident

laser power and the degree of mechanical damping at ambient and partial pressures; micro-mirror flatness, element size, and pitch; angular field-of-regard (FOR); bandwidth; scalability; and the angle/voltage transfer function. (FOR is a measure of the maximum angular extent to which the beamsteering element can steer an optical beam.) Measurements of these parameters for the MEMX device indicate that our application requirements can be met. For example, the angular FOR was approximately $\pm 7.9^\circ$ optical (whereas $\pm 12^\circ$ is projected for GEO-to-ground links), angular resolution was less than $360 \mu\text{rad}$ (whereas $<1000 \mu\text{rad}$ is required before the beam expansion optics), bandwidth was approximately 1 kHz (ideally, 100–1000 Hz), and mirror flatness was approximately 0.4 m (nominally ≈ 0.5 m), with a 10% variation from unit to unit.

We have recently implemented a simple image-based tracking system using a single MEMS mirror in conjunction with a fiber-coupled laser diode and CMOS camera, as shown in Fig. 9b.⁹ (A CMOS camera is a focal plane array technology similar to charge-coupled device camera technology, but it does not require shift registers to read out the photo-induced charge pattern, making it more versatile for sub-windowing portions of the entire image frame for tracking purposes.) We believe the MEMS technology can be scaled to a multichannel design for point-to-multipoint links and plan further work to develop a practical (space-worthy) multichannel beamsteering design.

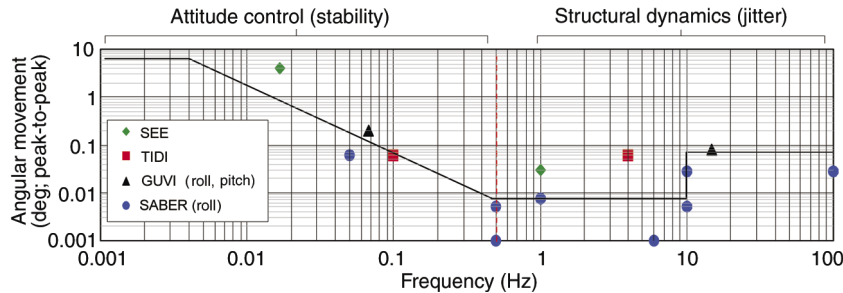


Figure 6. Example of nominal spacecraft angular vibration movement in degrees (peak-to-peak) versus frequency, showing the domains of attitude control at low frequencies and structural dynamics or jitter at higher frequencies. Most of the motion of concern for fine steering compensation for optical communications lies in the frequency range from 1 to 100 Hz. (SEE, TIDI, GUVI, and SABER are specific instruments on the TIMED spacecraft.)

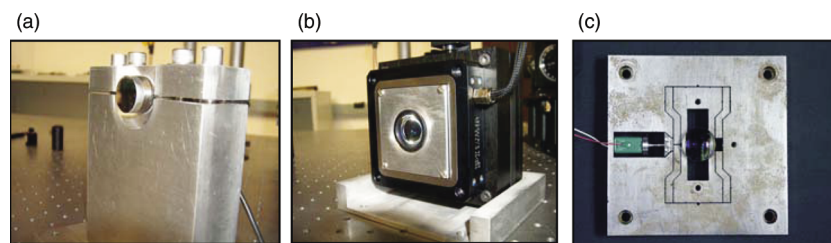


Figure 7. Beamsteering technologies: (a) Two-axis macro-tip/tilt mirror, (b) two-axis macro-translation stage, and (c) single-axis mesoscale translation stage. All are driven by piezoelectric actuators. The first two are COTS components, and the mesoscale component was developed by the National Institute of Standards and Technology (NIST).

Optics: Ultra-lightweight Large-aperture Cassegrain Telescope

We have recently begun to address the design and development of large-aperture lightweight telescopes for spacecraft-based optical communications.¹⁰ Large-aperture ultra-lightweight optical telescopes are especially desirable for very deep space optical communications. Diffraction-limited apertures 30–100 cm in diameter are compatible with high pointing accuracies ($\leq 1 \mu\text{rad}$) and a 10-mrad FOR. Compact deployable telescope designs are also desirable that can meet the above-mentioned angular accuracy and diffraction-limited performance requirements. Self-metering designs that incorporate active controls for image motion compensation and high-accuracy stabilization are being investigated at APL. A commercial

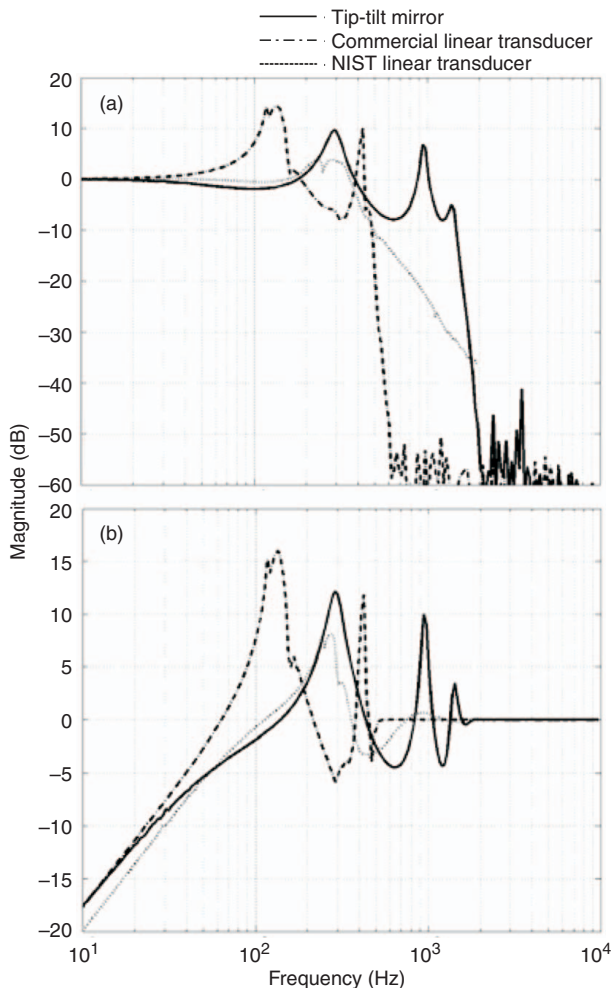


Figure 8. (a) Relative frequency response of the three actuators shown in Fig. 7 and (b) their corresponding rejection response to an input spectrum typical of spacecraft platform jitter. Although each actuator has a unique response, they generally have a low-pass characteristic with one or more resonances below the cutoff. The critical issues for control are to compensate for any mechanical resonances that would cause an underdamped response and to have a cutoff frequency sufficiently high to compensate for the majority of the platform jitter spectrum. The rejection response estimates the ability of each actuator to do this.

telescope test bed enabled us to verify deployment operation and control system correction of the secondary-to-primary misalignment errors, which included tip/tilt and piston errors (misfocus). A preliminary test article is shown in Fig. 10a and its collapsed configuration in Fig. 10b.

Results to date indicate that tip/tilt and piston control can be achieved to the accuracy required to support a deployable telescope design with a 1- μ rad pointing accuracy and a dynamic range sufficient to correct up to 1 mrad, the latter being within the state of the art for three-axis stabilized spacecraft attitude control systems. However, the accuracy results (lower bound) can probably be improved upon by a factor of ≈ 5 to support very accurate beamsteering for very deep space missions. The principal errors observed in this structure were

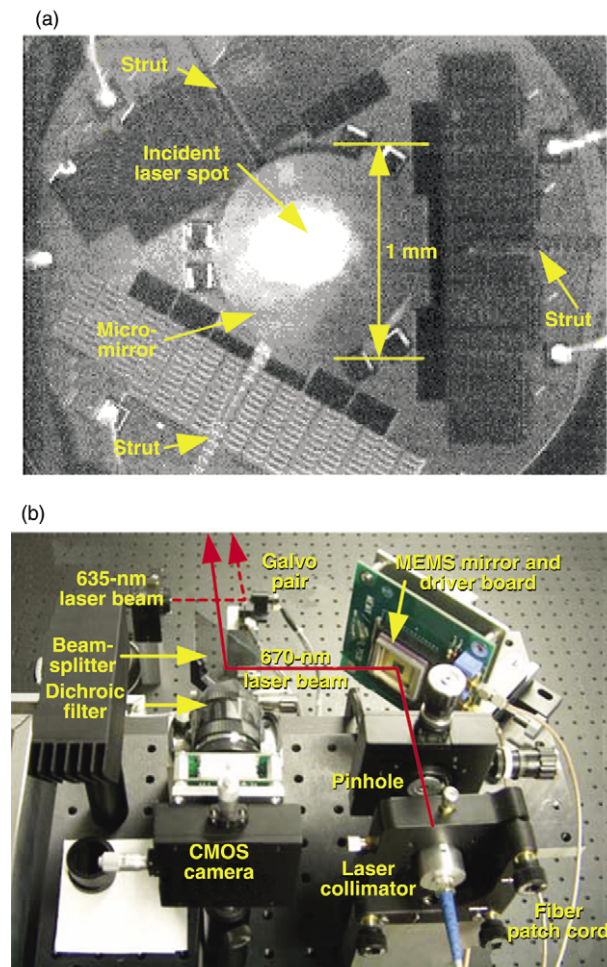


Figure 9. (a) MEMS micro-mirror developed by MEMX Corporation for use in optical switching, shown here under test at APL in an optical beamsteering experiment, and (b) a MEMS micro-mirror inserted into an optical tracking system. The optical tracking experiment (b) demonstrated that a target laser beam spot (at 635 nm) reflected off a white surface could be tracked by the CMOS camera and used to steer the target beam with a track beam (at 670 nm) employing a digital controller and a MEMS micro-mirror.

thermally induced, whereas mechanical vibrations caused less focus error. Deployment misalignments were very small and correctable. Several component improvements are foreseeable, including introducing an actual composite Cassegrain telescope, combining the tip/tilt and piston actuators into one transducer, reducing the digital signal processing controller to an FPGA chip for actual spacecraft implementation, and making the longerons from materials with low coefficients of thermal expansion.¹¹

THE FUTURE

The ultimate goal of the technology development described in this article is the implementation of an actual spacecraft optical communications terminal with minimum risk. In previous studies we have developed

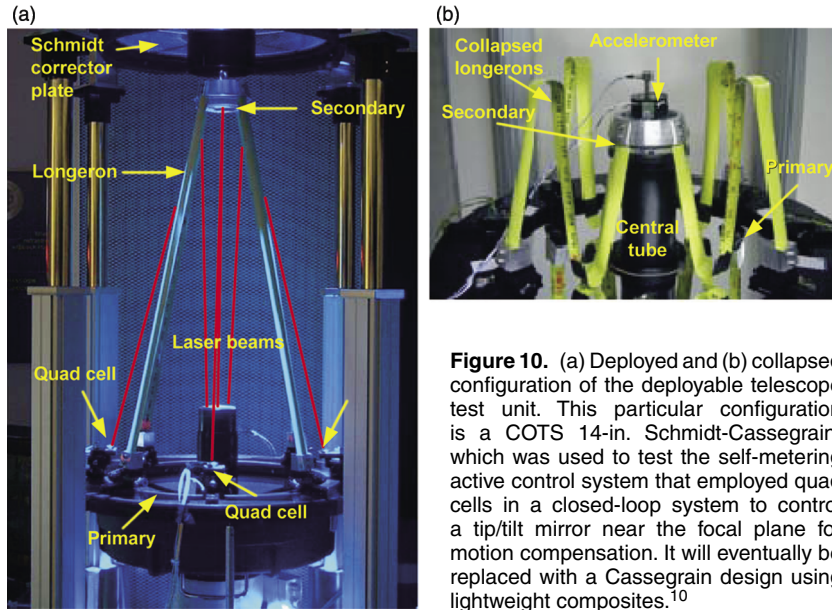


Figure 10. (a) Deployed and (b) collapsed configuration of the deployable telescope test unit. This particular configuration is a COTS 14-in. Schmidt-Cassegrain, which was used to test the self-metering active control system that employed quad cells in a closed-loop system to control a tip/tilt mirror near the focal plane for motion compensation. It will eventually be replaced with a Cassegrain design using lightweight composites.¹⁰

alternate approaches to the concept of a deep space optical communications terminal that has low mass prime power so that it can be used on smaller spacecraft typical of APL missions within the inner solar system or perhaps for very long-range missions¹² such as the Realistic Interstellar Explorer (RISE). A recent revision of the RISE mission sets its range at 200 AU. Our latest design concept builds upon previous studies in which a large diffractive membrane telescope was envisioned to reduce mass while achieving a meter-class aperture. This more recent design will use a more conservative composite Cassegrain structure that would also serve as an RF antenna. This concept is illustrated in Fig. 11, shown embedded in a notional spacecraft bus.

The design uses a dual-band primary in which the carbon fiber primary underlying substrate is reflective at X- or Ka-band but has a highly reflective, optically smooth metal coating with a low RF loss. Thus it would reflect both the microwave transmitter beam from a direct feed horn behind the secondary as well as a high peak power laser transmitter beam from a source behind the primary. The center hole of the primary will need to have an RF-reflective but optically transparent (dichroic) vertex plate, probably made from either indium tin oxide or perhaps a more exotic resonant tunneling metal-dielectric multilayer film. The secondary must also be dichroic but with properties complementary to those of the vertex plate so that it will reflect well optically but transmit with

minimal loss at the microwave frequency. The secondary surface will likely consist of a frequency-selective pattern to enable this. In addition, the RF feed horn may need a dielectric lens to adjust the RF beam to collimate it when it reflects off the shallow-sag primary dish.

A preliminary mass budget for this configuration is summarized in Table 1, although the RF feed horn mass is not included. The secondary optics includes the actual secondary mirror plus the imaging lens, laser beam expander, and relay optics. The optical communications system characteristics are summarized in Table 2. The laser power required for the optical link from 200 AU is well within the state of the art for fiber lasers except for the actual

peak power, which for a 100-ns slot time is just beyond the state of the art by about a factor of 3.

Tracking for deep space optical communications may be accomplished at sufficiently close ranges based on a beacon but at very long deep space link ranges, fully autonomous star tracking is the preferred approach. We have looked at both. We investigated a fully autonomous star tracking algorithm that was based on the principle of using patterns of stars in a series of unique pairwise configurations¹³ known as Golomb distributions. By comparing these unique patterns with the Tycho II star database we were able to show that accuracies approaching a few microradians are possible over a field of view of $\approx 1^\circ \times 1^\circ$ using stars down to approximately 10th magnitude with a 1-megapixel focal plane array and centroid tracking. Such a scheme would be suitable on a very deep space optical communications link such as that

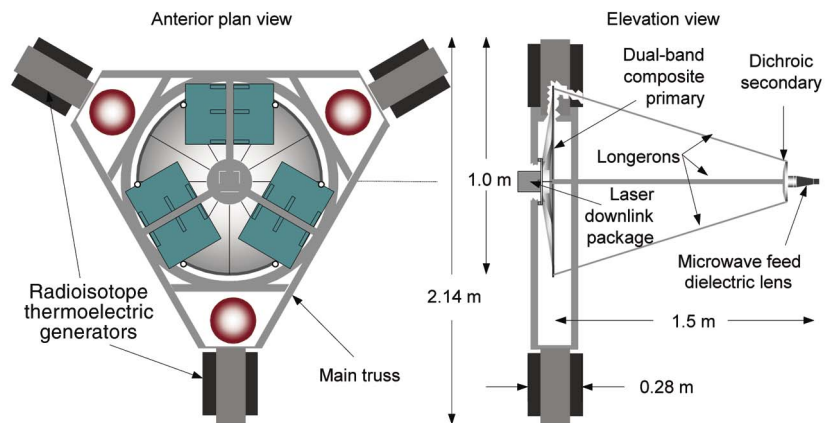


Figure 11. Notional RISE spacecraft design showing placement and configuration of the high-gain RF and optical communications antenna.

Table 1. Optical communications system mass budget for RISE.

Subsystem	Mass (kg)
Primary	5.2
Secondary optics	0.3
Structure	2.5
Electronics	2.0
Laser	3.5

associated with the RISE discussed earlier. Of course, in addition to the star tracker, an inertial measurement unit and periodic Earth ephemeris clock updates are required.

CONCLUSIONS

The goal of our strategic vision is to develop all the critical components of an optical communications terminal for spacecraft use in which its mass is kept to a minimum and its data rate falls within the range required to give a significant gain over an RF system, as summarized in Fig. 1. The Mars Laser Communication Demonstration, as currently envisioned, has a goal of 30 Mbps from Mars, but under frequent daylight receiver background conditions it will be much lower than this and just barely competitive with the RF downlink data rate, which is at best a few Mbps.

Table 2. Optical communications system characteristics.

Component	Rate
Spacecraft downlink transmitter (fiber laser source)	
Wavelength	1060 nm
Wall-plug efficiency	40%
Transmit aperture	1 m
Pointing accuracy	400 nrad
Communications link	
Data rate	500 bps
Bit error rate	10^{-6}
Modulation format	256-ary PPM
Slot width	100 ns
Forward error correction gain	10 dB
Link margin	3 dB
Ground receiver (avalanche photodiode)	
Background level	$7.3 \times 10^{-4} \text{ W/m}^2/\text{sr/nm}$
Receive aperture	5 m
Spectral bandpass	0.1 nm
Required transmitter power	
Peak power	102 kW
Average power	600 mW
Prime power	1.6 W

The pointing accuracy required to support a given mission is driven primarily by diffraction consistent with the desired link margin. For a meter-class aperture, this is a little less than 400 nrad as assumed in Table 2. These two factors, receiver sensitivity at the Earth terminal and pointing accuracy at the spacecraft, present the greatest technical challenge to future development and successful implementation of optical communications for deep space.

REFERENCES

- Boone, B. G., and Davidson, F. M., *High Data-Rate Communications IR&D Interim Report: Assessment of Optical Communication Technology for Spacecraft Applications*, Technical Memo. SER-01-032, JHU/APL, Laurel, MD (10 Jun 2001).
- Edwards, B. L., Townes, S. A., Bondurant, R. S., Scozzafava, J. J., Boroson, D. M., et al., "Overview of the Mars Laser Communications Demonstration Project," in *Proc. AIAA Space 2003 Conf.*, Long Beach, CA (Sep 2003).
- Hahn, D. V., Edwards, C. L., and Duncan, D. D., "Link Availability Model for Optical Communications Through Clouds," in *Proc. SPIE, Vol. 4821, Free-Space Laser Communications and Laser Imaging II*, Symp. on Optical Science and Technology, SPIE 47th Annu. Mtg., Seattle, WA, pp. 320–331 (7–11 Jul 2002).
- Hahn, D. V., and Duncan, D. D., "Optimized Link Model for Optical Communications Through Clouds," in *Proc. SPIE, Vol. 5550, Free-Space Laser Communications and Laser Imaging IV*, Symp. on Optical Science and Technology, SPIE 49th Annu. Mtg., Denver, CO (2–6 Aug 2004).
- Bruzzi, J. R., Boone, B. G., Millard, W. P., Connelly, J. R., and Liu, J., "Development of a Laser Transceiver System for Deep-Space Optical Communications," in *Proc. SPIE, Vol. 4821, Free-Space Laser Communications and Laser Imaging II*, Symp. on Optical Science and Technology, SPIE 47th Annu. Mtg., Seattle, WA, pp. 202–213 (7–11 Jul 2002).
- Koplow, J., Kilner, D. A. V., and Goldberg, L., "Single-mode Operation of a Coiled Multimode Fiber Amplifier," *OSA Optics Lett.* **25**(7), 442–444 (1 Apr 2000).
- Fielhauer, K. B., Boone, B. G., Bruzzi, J. R., Kluga, B. E., Connelly, J. R., et al., "Comparison of Macro-Tip/Tilt and Meso-Scale Position Beam-Steering Transducers for Free-Space Optical Communications Using a Quadrant Photodiode Sensor," in *Proc. SPIE, Vol. 5160, Free-Space Laser Communications and Active Laser Illumination III*, Symp. on Optical Science and Technology, SPIE 48th Annu. Mtg., San Diego, CA, pp. 192–203 (3–8 Aug 2003).
- Gorman, J. J., Dagalakis, N., and Boone, B. G., "Multi-loop Control of a Nanopositioning Mechanism for Ultra-precision Beam-steering," in *Proc. SPIE, Vol. 5160, Free-Space Laser Communications and Active Laser Illumination III*, Symp. on Optical Science and Technology, SPIE 48th Annu. Mtg., San Diego, CA, pp. 170–181 (3–8 Aug 2003).
- Sniegowski, J., Rodgers, S., Boone, B. G., Bruzzi, J. R., Drabenstadt, C. W., et al., "Development, Test and Evaluation of MEMS Micro-Mirrors for Free-space Optical Communications," in *Proc. SPIE, Vol. 5550, Free-Space Laser Communications and Laser Imaging IV*, Symp. on Optical Science and Technology, SPIE 49th Annu. Mtg., Denver, CO (2–6 Aug 2004).
- Boone, B. G., Bruzzi, J. R., Kluga, B. E., Rogala, E. W., Chen, P. C., and Hale, R. D., "Development and Testing of an Actively Controlled Large Aperture Cassegrain Telescope for Spacecraft Deployment," in *Proc. SPIE, Vol. 5487, Optical, Infrared, and Millimeter Wave Space Telescopes*, Symp. on Astronomical Telescopes and Instrumentation, Glasgow, Scotland, pp. 1042–1053 (21–25 Jun 2004).
- Chen, P. C., Bowers, C. W., Content, D. A., Marzouk, M., and Romeo, R. C., "Advances in Very Lightweight Composite Mirror Technology," *Opt. Eng.* **39**(9), 2320–2339 (2000).
- Boone, B. G., Bokulic, R. S., Andrews, G. B., McNutt, R. L. Jr., and Dagalakis, N., "Optical and Microwave Communications System Conceptual Design for a Realistic Interstellar Explorer,"

in *Proc. SPIE, Vol. 4821, Free-Space Laser Communications and Laser Imaging II*, Symp. on Optical Science and Technology, SPIE 47th Annu. Mtg., Seattle, WA, pp. 225–237 (7–11 Jul 2002).

¹³Maurer, D. E., and Boone, B. G., “Conceptual Design and Algorithm Evaluation for a Very Accurate Imaging Star Tracker for Deep-Space Optical Communications,” in *Proc. SPIE, Vol. 4821, Free-Space Laser Communications and Laser Imaging II*, Symp. on Optical Science and Technology, SPIE 47th Annu. Mtg., Seattle, WA, pp. 237–247 (7–11 Jul 2002).

ACKNOWLEDGMENT: The work reported in this article was supported by APL Independent Research and Development funds in the civilian space, military space, and exceptional science and technology business areas, as well as with funds from the NASA Institute for Advanced Concepts (NIAC). The authors would like to personally thank the following people for their support and guidance: Tom Krimigis, M. Lee Edwards, Robert Gold, Ralph McNutt, Paul Ostdiek, Dan McMorrow, Victor McCrary, Frederick M. Davidson, and Tom Strikwerda.

THE AUTHORS

The team for Optical Communications Development for Spacecraft Applications is led by **Bradley G. Boone**, who has been the Principal Investigator (PI) for the IR&D projects for most of the efforts described in the article. Dr. Boone is a member of the Principal Professional Staff and provides overall direction for the optical communications system conceptual design and component technology development, test, and evaluation efforts. **Jonathan R. Bruzzi** has assisted Dr. Boone and led algorithm and digital signal processing hardware development for optical modulation and demodulation as well as laser beamsteering and tracking. **Bernard E. Kluga** has provided the essential support for opto-mechanical and electronic hardware implementation for all aspects of the optical communications effort, especially the deployable telescope. **Wesley P. Millard** has provided expertise for optical communications modulator/demodulator hardware development. **Karl B. Fielhauer** has concentrated primarily on laser beamsteering and quadrant tracking algorithm development, test, and evaluation. **Donald D. Duncan** is an APL Principal Professional Staff member and has led theoretical and experimental efforts to evaluate atmospheric optical links. Dr. Duncan and **Daniel V. Hahn** are in the Electro-Optical Systems Group of APL's Air Defense Systems Department. They have focused on the effect of clouds on laser link bandwidth as well as fiber-to-telescope coupling issues. **Christian W. Drabenstadt**, who is in the Micro-electronics Group of the Technical Services Department with experience in photonics systems, has supported the evaluation of the MEMS beamsteering technology. **Donald E. Maurer** has provided important algorithm innovations. In addition, Dr. Maurer has conducted theoretical modeling of very accurate imaging star trackers that could support deep space optical downlinks. **Robert S. Bokulic** has complemented Dr. Boone in shaping the direction of optical communications efforts in the APL Space Department, including relevant system trade-offs and architecture design issues. Further information can be obtained through the PI, Brad Boone. His e-mail address is brad.boone@jhuapl.edu.



Bradley G. Boone



Jonathan R. Bruzzi



Bernard E. Kluga



Wesley P. Millard



Karl B. Fielhauer



Donald D. Duncan



Daniel V. Hahn



Christian W. Drabenstadt



Donald E. Maurer



Robert S. Bokulic